SOURCES OF BIAS IN PARTICLE-MESH METHODS FOR PDF MODELS FOR TURBULENT FLOWS

by

Jun Xu and Stephen B. Pope

FDA 97-01 January, 1997

Abstract

Numerical errors, in particular bias, in PDF-based particle-mesh methods for turbulence modeling have been explored. It is shown that bias decreases linearly with the increase of the number of particles, but increases with grid refinement. The fluctuations in mean fields which are fed back into the coefficients of stochastic differential equations are attributed to be the sources of bias. The *Frozen Coefficient* approach has been proposed and adopted to pinpoint the sources of bias in detail. These results provide guidelines for improving the numerical accuracy of PDF models for turbulent flows.

INTRODUCTION

For complex turbulent reactive flows, probability density function (PDF) methods have been well developed and offer great potential [4] [5]. In the application of these methods, a particle-mesh method is used to solve a modeled equation for the evolution of a PDF, e.g., the joint velocity-frequency-composition PDF. This is a Monte-Carlo method in which the PDF is represented by a large set of particles distributed in the physical space. This space is divided into a number of cells in order to estimate the mean fields such as the mean velocity as a function of position. Such a method has been implemented in the PDF2DV code [8] which is a Fortran code to calculate the properties of statistically two-dimensional (plane or axi-symmetric) turbulent reactive flows using the joint velocity-frequency-composition PDF model. In the present work, numerical errors, in particular bias, in PDF2DV are investigated.

The numerical accuracy and convergence of PDF methods have been discussed by Pope [6] and Welton et.al. [9]. Usually, weak convergence, i.e., the convergence of expectations instead of the PDF, is sought for PDF methods. Four different types of numerical errors have been identified by considering estimating a mean quantity: statistical error, spatial discretization error, temporal discretization error and bias. The convergence of numerical solutions to the modeled equations, which are stochastic differential equations (SDE), requires that numerical errors vanish as the particle number per cell N tends to infinity, and as the time step Δt and grid size h approach to zero. It has been shown that statistical error (SE) scales as $1/N^{1/2}$ [6]. It is reasonable to postulate that temporal error and spatial error, behave as that in finite difference method, i.e., both vanish as Δt and h tend to zero for fixed N.

However, in early experiences with the PDF2DV code it has been observed that there appeared to be relatively large bias. The bias is the deterministic error resulting from using a finite number of particles. Its features in the PDF methods are not very clear yet. This study is devoted to understanding the behavior and the sources of bias in PDF2DV, which will provide one of the guidelines for improving the accuracy of the code.

The description of bias in PDF2DV is presented in the next section, and then the strategies for pinpointing the sources of bias is described in the following section. Two test cases are used to search for the sources of bias: stationary homogeneous turbulence and Couette flow. Results for these cases are discussed. Conclusions are drawn in the final section.

DESCRIPTION OF BIAS IN PDF2DV

Before presenting the behavior of bias in PDF2DV, the model equations and some numerical techniques are introduced. A Lagrangian approach is taken both in the modeling and in the numerical method which is a Monte-Carlo particle-mesh method. The fluid-particle possesses properties: velocity $\mathbf{u}^+(t)$ and turbulence relaxation rate (turbulence frequency) $\omega^+(t)$. These properties are then modelled by the corresponding stochastic processes $\mathbf{u}^*(t)$ and $\omega^*(t)$ based on the idea of the stochastic Lagrangian modeling approach [7]. (If combustion is considered, the stochastic models for scalar fields are needed.) In PDF2DV, $\mathbf{u}^*(t)$ evolves according to the simplified Langevin equation (SLM, [7])

$$d\mathbf{u}^*(t) = -\nabla\langle p\rangle dt - \left(\frac{1}{2}+\frac{3}{4}C_0\right)\Omega\left(\mathbf{u}^*(t)-\langle\mathbf{U}\rangle\right)dt + \left(C_0 k\Omega\right)^{1/2} d\mathbf{W}, \tag{1}$$

where $\mathbf{W}$ is Wiener process, $\omega^*(t)$ is solved by the Ito stochastic differential equation [2]

$$d\omega^* = -C_3\left(\omega^*-\langle\omega\rangle\right)\Omega dt - \langle\omega\rangle\omega^* S_\omega dt + \left(2C_3\sigma^2\Omega\omega^*\langle\omega\rangle\right)^{1/2} dW. \tag{2}$$

The non-dimensional source term S_ω is defined as:

$$S_\omega = C_2 - C_1 S_{ij}S_{ij}/\langle\omega\rangle^2, \tag{3}$$

where S_{ij} is the mean rate of strain. For all other terms, model constants and the definition for conditional mean of turbulence frequency Ω in (1) and (2), refer to [2] [7].

In PDF2DV, the expectation of a random variable, e.g. $\langle\mathbf{U}\rangle$, is approximated by an ensemble mean estimated by the cloud-in-cell method. Because the number of samples, i.e., the number of particles per cell N is finite, the ensemble mean itself is a random variable. Of course, it also depends on time step Δt and grid size h. Several numerical techniques, e.g., variance reduction (VR) and time averaging (TAV), are adopted to reduce the statistical fluctuations in the mean fields [8].

The bias B_Q of a statistics $\langle Q\rangle$, e.g. $\langle U\rangle$, is the deterministic error caused by N being finite. Using $\langle Q\rangle_{N,\Delta t,h}$ to represent the ensemble-average of Q calculated by finite N, Δt and h, B_Q can be written as,

$$B_Q = \langle\langle Q\rangle_{N,\Delta t,h}\rangle - \langle Q\rangle_{\infty,\Delta t,h}. \tag{4}$$

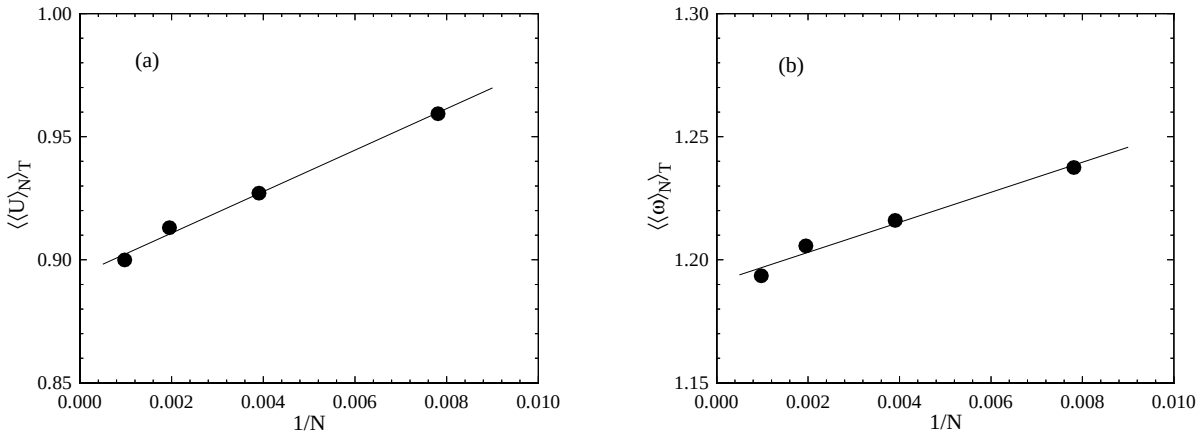

Figure 1: Time-averaged mean values vs. N in Couette flow: (a) Mean Velocity; (b) Mean $\langle\omega\rangle$. Grids in y direction $N_g = 21$, both VR and TAV are off, $y/H = 0.033$.

A simple analysis by Pope [6] suggests that bias B_Q scales as N^{-1}, so B_Q can be expressed as:

$$B_Q = \frac{b}{N}, \tag{5}$$

where b may be a function of other factors affecting bias, e.g., grid size and other numerical techniques in the code.

As an example, Couette flow (for flow descriptions refer to appendix A) is calculated using PDF2DV. With the same grid size, time step and numerical techniques, the time averages $\langle\langle U\rangle_N\rangle_T$ and $\langle\langle\omega\rangle_N\rangle_T$ of one point, which are equivalent with the ensemble mean of $\langle U\rangle_N$ and $\langle\omega\rangle_N$ respectively according to the ergodic assumption, are shown in Figure 1 as a function of the number of particles per cell. Since temporal error and spatial error are independent of particle number, the linear relationship in the figure implies that bias scales as (5). This behavior of bias is common in PDF2DV. The scale of bias as (5) ensures that bias approaches zero as N goes to infinity and thus leads to convergence of the scheme with respect to particle number per cell.

On the other hand, the slopes of the lines in Figure 1 provide the value of b in (5) which determines the magnitude of bias. For specific Δt and h (and for all other aspects of the

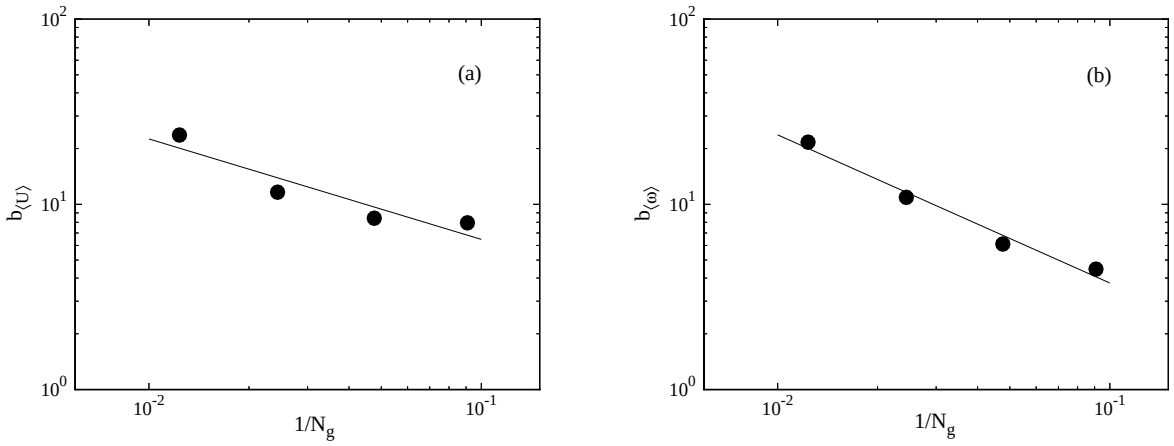

Figure 2: Bias vs. grid size in Couette flow: (a) Mean Velocity, the slope is -0.55; (b) Mean $\langle\omega\rangle$, the slope is -0.80. Both VR and TAV are off, $y/H = 0.033$.

numerical method fixed), we have

$$\langle Q\rangle_{N_1,\Delta t,h} - \langle Q\rangle_{N_2,\Delta t,h} = B_{Q_{N_1}} - B_{Q_{N_2}} = b\left(\frac{1}{N_1} - \frac{1}{N_2}\right), \tag{6}$$

A formula for b is thus obtained

$$b(\Delta t, h) = \frac{N_2 N_1}{N_2 - N_1}\left(\langle Q\rangle_{N_1,\Delta t,h} - \langle Q\rangle_{N_2,\Delta t,h}\right). \tag{7}$$

Consequently, using two different particle numbers per cell, b and B_Q can be calculated for a specific grid size. By fixing the time step and the numerical techniques, b for different grid sizes in Couette flow is obtained by (7) and is plotted against $1/N_g$ in Figure 2, where N_g is the number of cells or grids in the domain. Since nonuniform grids are used in this calculation, $1/N_g$ is used here to represent the averaged grid size. Figure 2 shows that b increases with grid size. This behavior is observed in homogeneous stationary turbulence (described in appendix A) as well. In this case, bias is the deviation of turbulence energy and turbulence frequency from the stationary solutions. As shown in Figure 3, increasing the number of cells results in larger bias.

The fact that the bias increases with grid size is of great concern to PDF2DV. If b explodes faster with grid size than the convergence of bias due to increasing N, bias will not

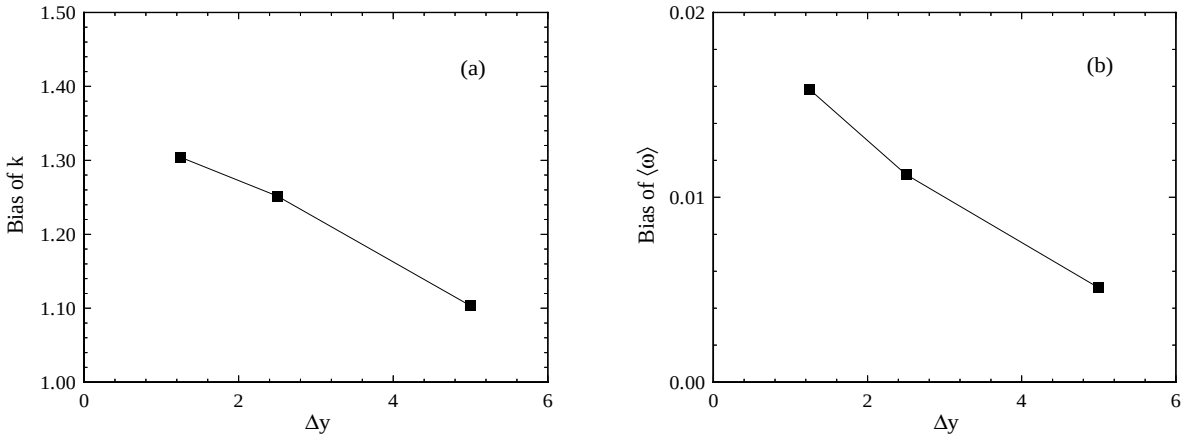

Figure 3: Bias vs. grid size in Homogeneous Stationary Turbulence: (a) Turbulence Energy k; (b) Mean $\langle\omega\rangle$. Time step $\Delta t = 0.1s$, for 4000 steps.

vanish as h approaches zero and N goes to infinity. In the view of numerical computations, to minimize the total numerical error, one might want to increase N_g to reduce the spatial discretization error, which unfortunately causes larger bias. Therefore, N must increase as N_g increases in order to prevent the bias from exploding and to get the total error converged, which thus leads to unacceptably high computational cost.

STRATEGIES FOR EXPLORING BIAS

Theoretically, the statistical fluctuations in the coefficients of the stochastic differential equations, e.g., the Langevin equation, are the major sources of bias. The numerical solutions to (1) and (2) are essentially different from the following standard problem: given coefficients $a(x,t)$ and $b(x,t)$, an initial condition $X(0) = x_0$, and a stopping time $T > 0$, integrate the stochastic differential equation

$$dX(t) = a(X(t),t)dt + b(X(t),t)dW(t), \tag{8}$$

which has been well studied [3]. This is because in (1) and (2), the coefficients depend on the mean of a function of the process, e.g., $\langle \mathbf{U} \rangle$, which needs to be estimated in numerical

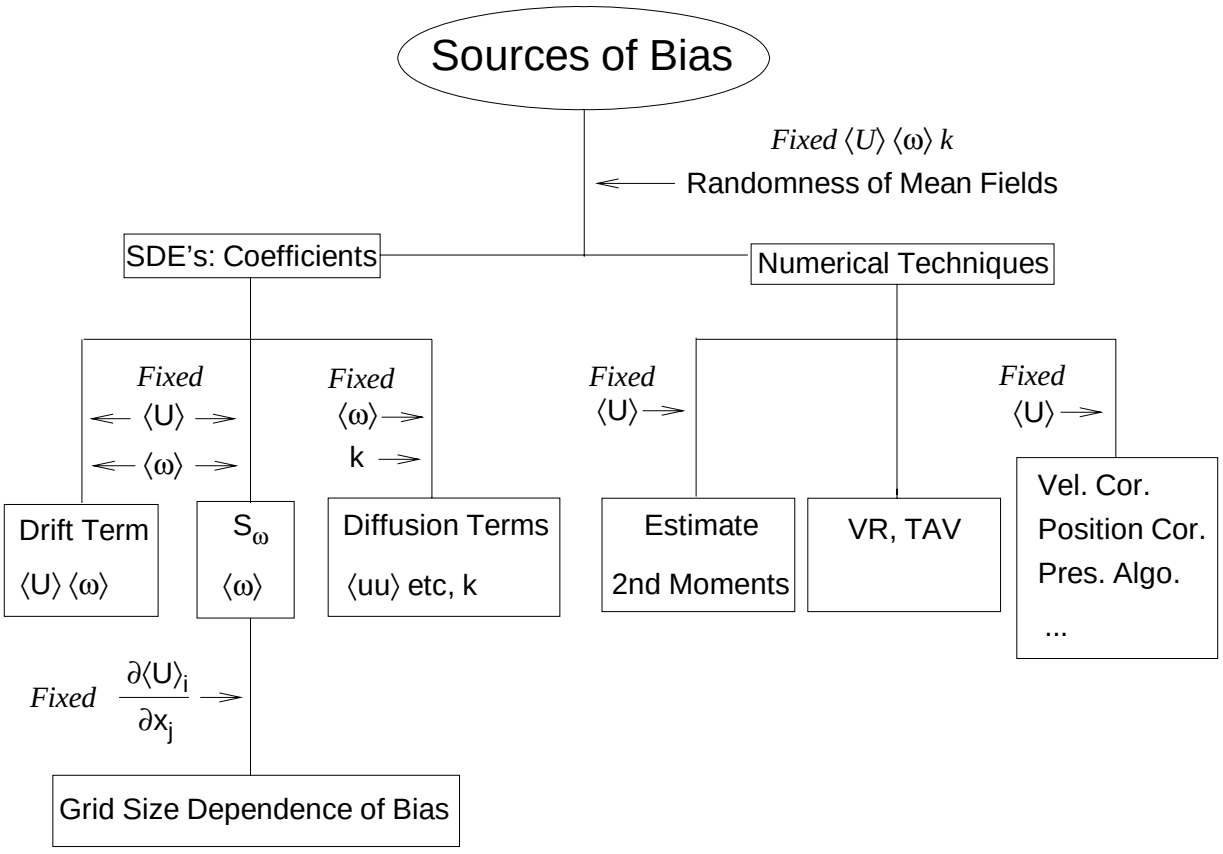

Figure 4: Strategies for exploring bias in PDF2DV

computation and inevitably carries numerical fluctuations. The mean fields in PDF2DV are calculated by cloud-in-cell method and fed back into the coefficients. This feedback causes bias. The two questions to be addressed are:

1. Which coefficients associated with mean fields yield bias ?

2. Why does bias increase with finer grids ?

For the PDF2DV code, all mean fields, terms in the SDE's and numerical techniques which may be related to the above two issues are sketched in Figure 4.

If, instead, the coefficients were non-random, independent of particle properties, the computed particle properties at any time would be independent, identically distributed,

and independent of N. It follows then there would be no bias. Therefore, if the estimate of mean field is replaced by a non-random input (say fixed or frozen $\langle U \rangle$), there is no corresponding statistical fluctuation in that mean field and related terms in the SDE's so that the contribution of statistical errors in the mean field to bias will be prevented. According to this *Frozen Coefficient* approach, a mean field or a term in the SDE's is justified as a source of bias if freezing it results in no bias. The things to be tested, which are possibly the sources of bias, and associated methods, are also shown in Figure 4.

NUMERICAL TESTS AND RESULTS

The approach of *Frozen Coefficient* is accomplished step by step through numerical tests. Because the fluctuations in the mean fields are suspected to be the major sources of bias, first of all the calculations are made by fixing mean fields in all coefficients of the SDE's to check the behavior of bias. If it disappears, then we can conclude that bias arises entirely from the fluctuations in the coefficients and no more calculations are needed to search for other sources of bias due to the numerical techniques. Several cases are calculated and compared to the base case; namely, the result from the original code without VR and TAV. The conditions for different cases are presented in Table I.

1 Sources of Bias: General Views

In the calculation of case 1, it is not the estimates from cloud-in-cell method that are used but constant values for mean fields. No bias is expected if bias is only related to the statistical fluctuations in the mean fields. The result compared to the base case (case 0) is shown in Table I. Obviously, bias of velocity and $\langle \omega \rangle$ are much smaller than case 0 and almost zero after fixing mean fields globally. Therefore bias of these two variables is because of the fluctuations in the estimates of mean fields. However, because the ensemble mean of velocity is used to estimate second moments, bias of turbulent energy is increased instead, which implies that the fluctuations in the first moments are the source of bias for the second moments. This will be discussed further in other cases.

2 Source of Bias for Velocity

Fixing Mean Fields for Coefficients in Eq.(1)

To clarify further that bias of velocity comes from Eq.(1), case 2 is calculated by fixing all mean fields in this equation. As in Table I, this case shows that the bias of the mean velocity is in the same order as case 1, which indicates that the bias of velocity is due to the fluctuations in the mean fields fed back into the coefficients of Eq.(1). This is consistent with the analysis in the previous section. To distinguish the influence on bias of drift term from diffusion term in Eq.(1), the following cases are designed.

Fixing Mean Velocity for Drift Term

The mean velocity is a critical variable in Eq.(1) because the particle velocity is forced to relax to it, and the particle velocity, in turn, is used to estimate the mean velocity. This means that there must be a very strong interaction between them. As shown in Table I (case 3), the bias of velocity resulting from fixing the mean velocity for the drift term in Eq.(1) is very small. Hence, the fluctuation in mean velocity is a major source for bias of velocity. One more interesting observation is that the bias of $\langle\omega\rangle$ becomes very small in this case as well. It seems that the behavior of the bias of $\langle\omega\rangle$ is dominated by the mean velocity although Eq.(2) is the same in the form as Eq.(1). This will be further discussed later.

It may be noticed that in case 3 there is a huge bias of k. However, this phenomenon should not be paid too much attention. When the drift term is frozen while the diffusion term is not, in the equation for k derived from Eq.(1), $-\frac{3}{4}C_0\Omega(\mathbf{u}^* - \langle\mathbf{U}\rangle)dt$ in the drift term will not still balance with the diffusion term, which may cause a large bias of k.

Fixing Ω and k

In order to determine the effect of fluctuations in the diffusion coefficients, a calculation was attempted in which Ω and k were fixed only in the diffusion term in Eq.(1). It turns out that the solution is not stable. The explanation could be that different values of Ω in the drift and diffusion terms give rise to an instability of numerical solutions to the equation. This case is then modified to let Ω take fixed values both for the drift term and the diffusion term

and k be fixed for the diffusion term so that a stationary solution is obtained. Thus, in this case 4, k and Ω (but not $\langle U \rangle$) are fixed throughout Eq.(1). The bias of velocity is almost the same as in case 0. The bias of $\langle \omega \rangle$ is not much reduced either. This case demonstrates that the diffusion term of Eq.(1) is not the source of significant bias for the velocity or for $\langle \omega \rangle$.

3 Source of Bias for $\langle \omega \rangle$

Fixing Mean Fields for Coefficients in Eq.(2)

In case 5, the coefficients in Eq.(2) are fixed. The bias of $\langle \omega \rangle$ is very small (Table I). Therefore, the bias of $\langle \omega \rangle$ stems from the fluctuations in the coefficients of Eq.(2).

Fixing Mean Velocity Gradient for Turbulent Frequency Equation

An analysis given in Appendix B shows that bias in the source term S_ω in the turbulent frequency model increases with grid refinement because of the fluctuations in the mean velocity. This may be the reason for the dependence of bias on grid size, which can be demonstrated by fixing the mean velocity gradient to calculate S_ω. The results in this case (case 7) are compared with the results of original model. Figure 5 shows that the dependence of bias on grid size almost disappears when a fixed mean velocity gradient is used to calculate S_ω. Therefore, the reason that bias increases when grid size are decreased is that the fluctuations in the mean velocity bring about an additional source into the turbulent frequency model because of the square of velocity gradient in S_ω. In addition to this observation, it is shown in Figure 5 and Table I that bias of $\langle \omega \rangle$ is almost zero. Consequently, the bias of $\langle \omega \rangle$ is dominated by the fluctuations in the mean velocity.

4 Source of Bias for Turbulent Energy k

Homogeneous Flow: Fixing Mean Velocity for Estimate of Second Moments

In this case (case H-1 in Table II), the fixed no-random first moment (the mean velocity) is used to estimate second moments. Table II shows that bias reduces by about half in

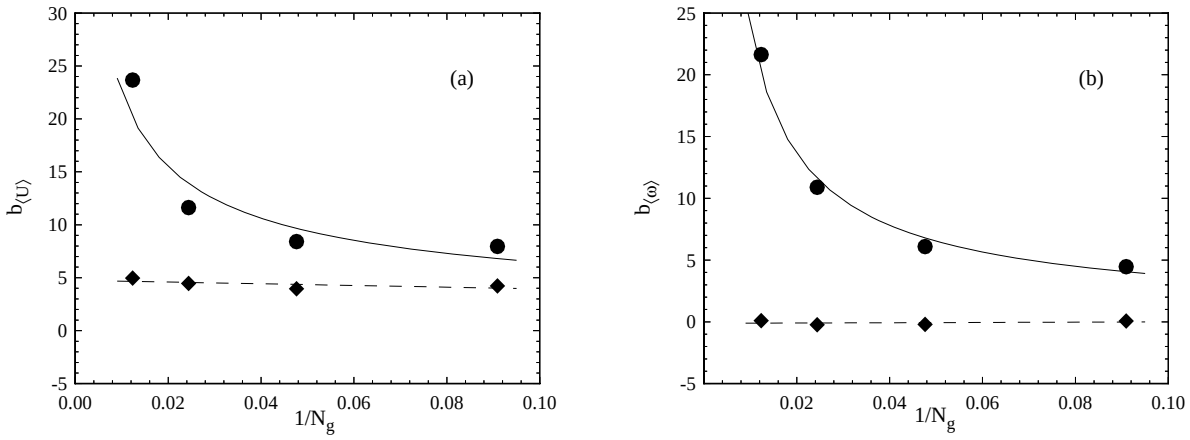

Figure 5: Comparison of the dependence of Bias on grid size in Couette flow: (a) Mean Velocity; (b) Mean $\langle\omega\rangle$; solid line, base case (case 0); dashed line, calculation by fixing velocity gradient (case 7). Both VR and TAV are off, $y/H = 0.033$.

comparison with case H-0. As pointed out before, the fluctuations carried by first moments are the sources of bias for k.

Couette Flow: Fixing k for Diffusion Term

This case is to test whether the fluctuation in k which is fed back into the diffusion term of Eq.(1) is the source of bias in k or not. The result is shown in Table I (case 6). Apparently, fixing k for the diffusion term does not reduce the bias of k. Case 4 shows, however, that by fixing both Ω and k in diffusion term, bias of k is indeed reduced. Therefore, the diffusion term is a source of bias in k due to the fluctuations in both Ω and k.

Homogeneous Flow: Fixing Mean Velocity for Estimate of Second Moments and Ω, k for Eq.(1)

The case H-2 is calculated to clarify further that the total bias of k is contributed by the above sources: the fluctuations in the first order moments which are used to estimate the second moments; the fluctuations in Ω and k which are feeded back into Eq.(1) (Table II).

Table I: Bias in Couette Flow: Test Cases and Results

Cases		0	1	2	3	4	5	6	7	8
Drift Term in the	$\langle U \rangle$		×	×	×					
Equation for $\mathbf{u}^*$	Ω		×	×		×				×
Diffusion Term in	Ω		×	×		×				×
the Equation for $\mathbf{u}^*$	k		×	×		×		×		
Drift Term in the	Ω		×				×			
Equation for ω^*	$\langle \omega \rangle$		×				×			
Diffusion Term in	Ω		×				×			
the Equation for ω^*	$\langle \omega \rangle$		×				×			
Source Term S_ω in	$\frac{\partial \langle U \rangle}{\partial y}$		×				×		×	
the Equation for ω^*	$\langle \omega \rangle$		×				×			
Evaluation of k	$\langle U \rangle$									
Measurement	$b_{\langle U \rangle}$	8.42	0.14	0.23	0.37	7.70	3.94	21.53	3.95	5.58
of Bias	$b_{\langle \omega \rangle}$	6.10	-0.23	1.26	-0.96	4.85	0.38	10.03	-0.20	4.66
	b_k	0.6	-1.96	-2.76	-12.0	0.14	0.81	1.03	-0.03	-0.39

Note. All calculations are made on the conditions: $N_g = 21$, neither VR nor TAV, $y/H = 0.033$. b's are normalized by mean fields at the wall. '×' denotes the parameter is fixed.

Table II: Bias in Stationary Homogeneous Turbulence

Case	Description	Bias of k	Bias of $\langle \omega \rangle$
H-0	No any coefficients fixed	1.103	0.0051
H-1	Fix $\langle U \rangle$ for estimate of second moments	0.54	0.0071
H-2	Fix $\langle U \rangle$ for estimate of second moments and fix Ω, k for Eq.(1)	0.004	0.010

Note. All calculations are made on the conditions: $N_g = 3$, neither VR nor TAV, time step $\Delta t = 0.1s$, for 4000 steps.

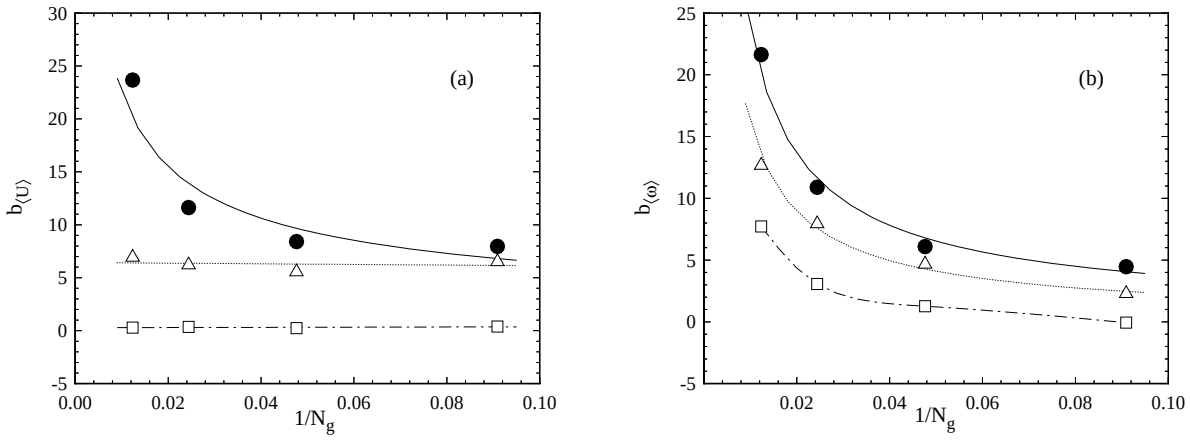

Figure 6: Comparison of the dependence of Bias on grid size in Couette flow: (a) Mean Velocity; (b) Mean $\langle\omega\rangle$; solid line, base case (case 0); dot-dashed line, calculation by fixing all mean fields for Eq.(1) (case 2); dotted line, calculation by fixing Ω for Eq.(1) (case 8).

5 Dependence of Bias on Grid Size

In the case of fixing velocity gradients for the turbulent frequency model, it has been shown that the source term S_ω in this model introduces the dependence of bias on grid refinement. Here two more cases are set up to confirm this further.

Fixing All Mean Fields for Eq. (1)

It has been shown in Table I that the bias of velocity almost disappears in this case (case 2). Here, it can be seen further from Figure 6 that the bias of velocity is apparently independent of the grid size while the bias of $\langle\omega\rangle$ still increases as the grid is refined.

Fixing Ω for Eq. (1)

By fixing Ω in Eq.(1), the contribution of the turbulent frequency model to the dependence of bias on grid refinement can be further clarified. In this case (case 8), the bias of $\langle\omega\rangle$ still increases with the grid refinement (Figure 6). In contrast, the bias of velocity does not exhibit such a behavior anymore.

From the above two cases and the case of fixing the velocity gradients for the turbulent frequency model, it can be concluded that the source term S_ω causes the bias of $\langle\omega\rangle$ to depend on the grid size and increase when the grid size is refined. Then, the bias of velocity is affected by $\langle\omega\rangle$ or Ω through Eq.(1) so that it increases with the finer grids as well.

6 Summarization

The sources of bias in the PDF2DV code have been summarized in Figure (7) which provides a general picture of the sources of bias.

CONCLUSIONS

In PDF particle-mesh methods for turbulence modeling, three types of numerical errors are identified: statistical error, truncation error, and bias. The behavior and the sources of bias in the PDF2DV code applying such a method have been studied in detail by numerical experiments.

It has been verified that bias is linearly proportional to N^{-1} so that bias decreases with increasing particle number, which is consistent with analysis. Another observation is that bias increases when the grid size is decreased. This is significant because it could lead to unacceptably high computational cost.

The *Frozen Coefficient* approach has been proposed to pinpoint the sources of bias in PDF2DV. According to this approach, the sources of bias are found through fixing or freezing the mean fields that appear in the stochastic differential equations, i.e. using non-random value instead of estimates by cloud-in-cell method. This procedure is implemented by isolating each term in the stochastic differential equations. The source of bias in velocity is found to be associated with the fluctuations in the estimated mean of velocity. In other words, the drift term in the Langevin equation for velocity is the major source of bias for velocity. As for the turbulent frequency $\langle\omega\rangle$, the bias is mostly dominated by the mean velocity and its gradient. On the other hand, the bias of second moments (or turbulence energy k) has two sources: the diffusion term of the Langevin equations for velocity which is related to the fluctuations in $\langle\omega\rangle$ and k, and the estimation of second moments based on the first moments

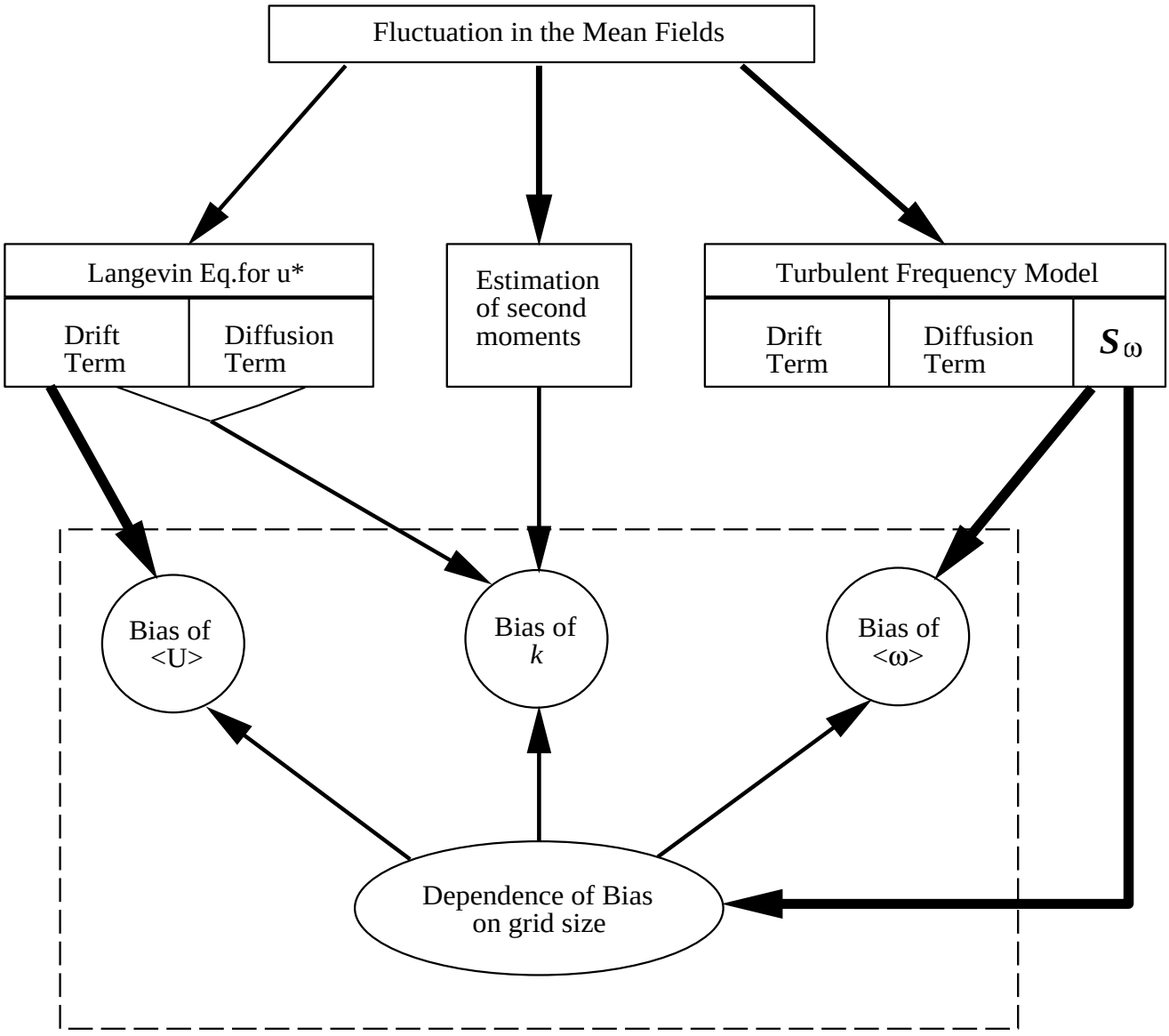

Figure 7: The chart describing the sources of bias

which of course carry fluctuations. Lastly, the dependence of bias on grid size has been attributed to the source term S_ω in the turbulent frequency model. The analysis also shows that the bias of S_ω increases with grid refinement. This leads to the dependence of bias of $\langle\omega\rangle$ and thus Ω on grid size, which furthermore affect the mean velocity through Eq.(1) so that it also depends on the grid size. The fact that bias increases as the grid size is decreased implies the PDF2DV code is not unconditionally convergent and is not acceptable.

Discovering the sources of bias provides a guideline for reducing bias and removing the dependence of bias on grid size. Partially time averaging, variance reduction techniques and modification of turbulent frequency model are possible approaches to improve the accuracy of this PDF particle method. This will be discussed in another report.

Acknowledgements

This work was suppported by the Air Force Office of Scientific Research, Grant F49620-94-1-0098.

APPENDIX A: TEST FLOWS

The test flows used in this study are Couette flow and stationary homogeneous flow. Both of them have the following features

(i) they are 0-D or 1-D problem,

(ii) they exhibit easily understandable physics, and

(iii) they are statistically stationary.

Because of these features, many calculations are feasible during a reasonable time; the sources of bias are distinguishable from other issues in the code and some numerical techniques, e.g. time-averaging, can be tested. The two flows are described in this appendix.

(1) Couette Flow

Couette flow is defined as the flow between two flat plates which move in the opposite direction at velocity U_w (Figure 8) . The flow is one dimensional. No pressure gradient in x direction is needed to drive the flow.

For such a flow, boundary conditions need to be defined on the wall. Since only the lower half of the domain is calculated, the boundary conditions are defined at the center line and at the lower wall. In the frame of a particle method, the physical condition is imposed through specifying the particle properties. The following boundary conditions for the particle may not give the exact solution to Couette flow. However, because we are mostly interested in the numerical features of PDF2DV, we can put aside the physical consistency of calculation with real world. The issues we are concerned with should be whether these conditions give a stable and stationary solution.

(a) Center Line

At the center line, the physical conditions are

$$\langle U \rangle = 0, \qquad \frac{\partial \langle uv \rangle}{\partial y} = 0, \tag{9}$$

and

$$\frac{\partial \langle \omega \rangle}{\partial y} = 0. \tag{10}$$

so that the particle conditions are imposed as

$$u_R^* \;\; = \;\; -u_I^*, \tag{11}$$

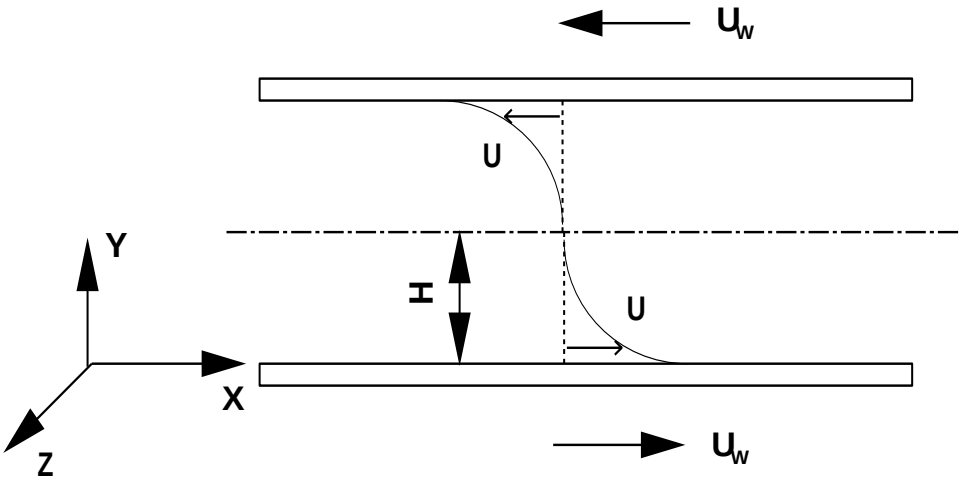

Figure 8: Couette flow configuration

$$v_R^* = -v_I^*, \tag{12}$$

$$\omega_R^* = \omega_I^*, \tag{13}$$

where 'I' denotes particles which are incident to the boundary and 'R' denotes particles which are "reflected" from the boundary. The mean conditions are obtained as the average of the condition before and after reflection. It can be shown readily that particle conditions are consistent with physical conditions.

(b) Wall Conditions

The boundary conditions at the wall are more difficult to define for particles than at the center line. A modified wall function proposed by Dreeben [1] is used in this study.

The conditions for the mean velocities are

$$\langle U \rangle = U_w, \quad \langle V \rangle = 0. \tag{14}$$

The velocities of particles hitting the wall satisfy the following conditions:

$$u_R^* = u_I^* + \alpha v_I^*, \tag{15}$$

$$v_R^* = -v_I^*, \tag{16}$$

where α can be calculated from the wall function. To be consistent with the mean conditions

at the wall, α must satisfy

$$\alpha = \frac{-2\langle uv \rangle_w}{\langle v^2 \rangle_w}, \tag{17}$$

where 'w' stands for values at the wall. Using the wall function, a formula for α can then be deduced,

$$\alpha = \frac{C_w \langle U \rangle_w / k_w^{1/2}}{\kappa U_w / \hat{u} - \ln(E\lambda\hat{u}/\nu)}, \tag{18}$$

where the friction velocity $\hat{u}$ is calculated by

$$\hat{u} = C_\mu^{1/4} k^{1/2}. \tag{19}$$

All other model constants are chosen as

$$C_\mu = 0.0841, \qquad \kappa = 0.4, \tag{20}$$

$$C_w = 0.76, \qquad E = 8.0, \tag{21}$$

$$\lambda = 0.05. \tag{22}$$

As for conditions for turbulence frequency at the wall, a modified form of the model proposed by Dreeben et.al. [1] is adopted. The particle condition is

$$\omega_R = e^{\beta \frac{V_I}{\lambda \langle \omega \rangle}} \omega_I. \tag{23}$$

Dreeben et.al. deduce the following formula for β [1]

$$\beta = \frac{-2\lambda \langle \omega \rangle \langle \omega v \rangle}{\langle \omega v^2 \rangle} + O(\beta^3). \tag{24}$$

Here a simplified form for β, i.e. a constant, is used

$$\beta = -0.5. \tag{25}$$

The above boundary conditions indeed yield a stable and stationary solution to Couette flow. The profiles of the mean velocity and the mean turbulence frequency from the above boundary conditions are shown in Figure 9.

(2) Stationary Homogeneous Turbulence

The coefficient $\left(\frac{1}{2} + \frac{3}{4}C_0\right)$ in SLM (Eq. (1)) causes the turbulence energy to be dissipated at the rate $\langle \epsilon \rangle$ or $k\langle \omega \rangle$. If the $\frac{1}{2}$ is omitted, the equation (1) will pertain to the hypothetical

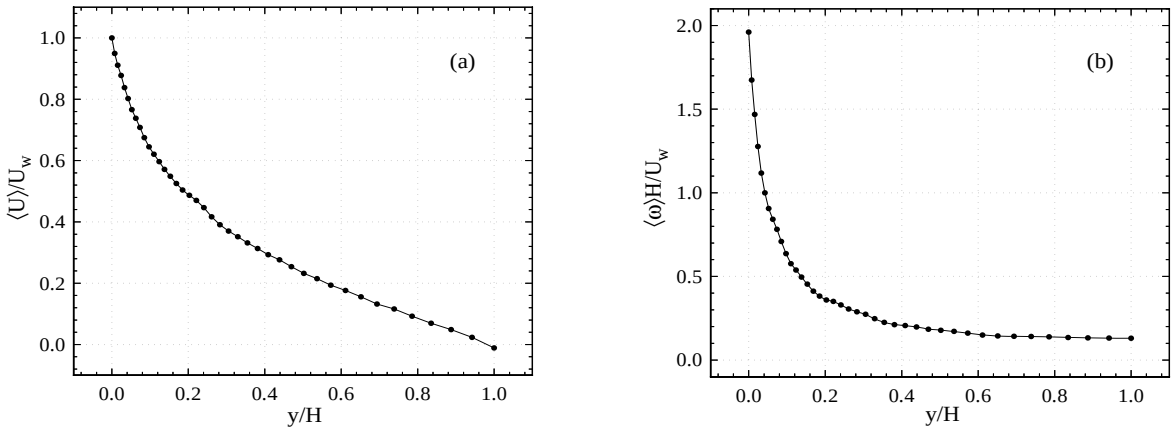

Figure 9: Calculated profiles of Couette flow: (a) Mean Velocity; (b) Mean $\langle\omega\rangle$. Calculation conditions: Half width of channel $H = 1$, Wall velocity $U_w = 1$, Grids in y direction $N_g = 41$

case of stationary (i.e. non-decaying) homogeneous (isotropic) turbulence. In this flow, as turbulence energy does not decay and there does not exist production either, theoretically the solutions to this flow are constant against time, i.e. stationary solutions are expected. To assure a stationary solution for $\langle\omega\rangle$ as well, in Eq.(3) constant C_2 is set to be zero. Because the mean rate of strain S_{ij} is zero (ideally), a stationary solution to $\langle\omega\rangle$ is expected. To see the effect of grid size on bias, we treat this flow as 1-D flow instead of 0-D, i.e. in one direction, say y direction, multiple grids instead of one grid are used.

APPENDIX B: DEPENDENCE OF BIAS IN S_ω ON GRID SIZE

As in Eq.(3), S_ω is involved with the square of the strain rate. In Couette flow and stationary homogeneous turbulence it reduces to

$$S_\omega = C_2 - \frac{1}{2}C_1\left(\frac{\partial\langle U\rangle}{\partial y}\right)^2\frac{1}{\langle\omega\rangle^2}. \tag{26}$$

In the numerical calculation, the differentiation is replaced by finite difference. According

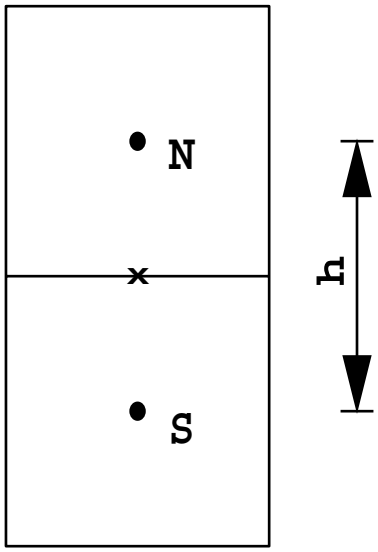

Figure 10: Cell and Node Structure

to Figure 10,

$$\left(\frac{\partial\langle U\rangle}{\partial y}\right)^2 \sim \left(\frac{\langle U\rangle_n - \langle U\rangle_s}{h}\right)^2. \tag{27}$$

And then, $\langle U\rangle$ is approximated by the corresponding ensemble mean $\{U\}$ estimated by cloud-in-cell method. The bias of $\left(\frac{\partial\langle U\rangle}{\partial y}\right)^2$ is defined as

$$B_{u,y} = \left\langle \left(\frac{\{U\}_n - \{U\}_s}{h}\right)^2 \right\rangle - \left(\frac{\langle U\rangle_n - \langle U\rangle_s}{h}\right)^2. \tag{28}$$

This can rewritten as

$$\begin{aligned}
B_{u,y} &= \left\langle \frac{\{U\}_n^2 + \{U\}_s^2 - 2\{U\}_n\{U\}_s}{h^2} \right\rangle - \frac{\langle U\rangle_n^2 + \langle U\rangle_s^2 - 2\langle U\rangle_n\langle U\rangle_s}{h^2}, \\
&= \frac{1}{h^2}\left(\langle\{U\}_n^2\rangle - \langle U\rangle_n^2\right) + \frac{1}{h^2}\left(\langle\{U\}_s^2\rangle - \langle U\rangle_s^2\right) - \frac{2}{h^2}\left(\{U\}_n\{U\}_s - \langle U\rangle_n\langle U\rangle_s\right), \\
&= \frac{1}{h^2}\left[Var(\{U\}_n) + Var(\{U\}_s)\right] - \frac{2}{h^2}Cov(\{U\}_n, \{U\}_s), \\
&= \frac{1}{h^2}\left[\sqrt{Var(\{U\}_n)} - \sqrt{Var(\{U\}_s)}\right]^2 + \frac{2}{h^2}\left[Var(\{U\}_n)Var(\{U\}_s)\right]^{1/2}(1-\rho), \\
&\geq \frac{2}{h^2}\left[Var(\{U\}_n)Var(\{U\}_s)\right]^{1/2}(1-\rho),
\end{aligned} \tag{29}$$

where ρ is the correlation coefficient between $\{U\}_n$ and $\{U\}_s$. In most of the cases, ρ is less than one, so bias of $\left(\frac{\partial\langle U\rangle}{\partial y}\right)^2$ or S_ω is not zero and determined by the variance of the estimate

of the mean velocity and the grid size. As far as there exists fluctuations in the estimate of the mean velocity, $B_{u,y}$ increases with grid size refinement. Consequently, the bias of S_ω depends on the grid size.

REFERENCES

[1] T.D. Dreeben and S.B. Pope. Wall-function treatment in pdf methods. *Physics of Fluids*, To be published.

[2] Jayesh and S.B. Pope. Stochastic model for turbulent frequency. Technical Report FDA 95-05, Cornell University, 1995.

[3] P.E. Kloeden and E. Platen. *Numerical Solution of Stochastic Differential Equations*. Springer-Verlag, 1992.

[4] S.B. Pope. Pdf methods for turbulent reactive flws. *Progress Energy and Combustion Science*, 11:119–192, 1985.

[5] S.B. Pope. Computations of turbulent combustion: Progress and challenges. In *Proceedings of the Twenty-Third Symposium on Combustion*, pages 591–612, 1990. Actual booktitle unknown.

[6] S.B. Pope. Particle method for turbulent flows: Integration of stochastic differential equations. *J. Comput. Phys.*, 117:332–349, 1992.

[7] S.B. Pope. Lagrangian pdf methods for turbulent flows. *Annual Review of Fluid Mechanics*, 26:23–63, 1994.

[8] S.B. Pope. *pdf2dv*. Cornell University, Sibley School of Mechanical Engineering, Ithaca, NY 14853, 1994.

[9] W.C. Welton and S.B. Pope. A PDF-based particle method for compressible turbulent flows. *AIAA Paper No. 95-0804*, 1995.